JMEPEG (2009) 18:216–220
DOI: 10.1007/s11665-008-9280-y

1059-9495/$19.00

Effects of Microstructure on Corrosion of X70 Pipe Steel in an Alkaline Soil

C.W. Du, X.G. Li, P. Liang, Z.Y. Liu, G.F. Jia, and Y.F. Cheng

(Submitted January 22, 2008; in revised form July 4, 2008)

Corrosion of X70 steel with different heat treatments (quenching, air cooling, and furnace cooling) in an alkaline soil was investigated by weight-loss, surface characterization and electrochemical measurements. The cathodic/anodic reactions of X70 steel in alkaline soil are dominated by the oxygen reduction and formation of iron oxides that deposit on the steel surface. The protection of the oxide deposit is through a physical block effect. The deposit layer formed on as-received steel has a compact, complete structure and thus, provides an effective protection over the underneath steel. However, the deposit layers on the heat-treated steels are generally loose, porous and defective, and provide minor protectiveness. Corrosion of steel is affected by its microstructure. Generally, steels with heat treatments have a higher corrosion rate than the as-received steel. The presence of more pearlite enhances the corrosion rate of ferrite by a galvanic effect. When the steel contains bainite and martenite phases, the activity of the steel is further increased.

Keywords corrosion, microstructure, soil, X70 steel

1. Introduction

API grade X70 steel has been used extensively in high-pressure natural gas transmission in China. Several research projects have been performed to investigate corrosion and stress corrosion cracking (SCC) of X70 steel as well as the associated coating degradation in the various soil environments (Ref 1-5).

Welding is the main method for pipeline connection and repair. Generally, welding would result in changes in microstructure and mechanical strength of the welded area compared to the matrix steel. Consequently, the corrosion and SCC behavior of the weld is expected to be different from the steel in soil. It is thus essential to investigate the effects of microstructural changes associated with welding operation on corrosion of X70 steel.

Salt lakes are widely distributed in North-West China, where soil salinization is a vital threat to the integrity of buried pipelines and other metallic facilities. There have been some preliminary researches conducted to study corrosion of steels in such a highly saline soil (Ref 6-8). However, a systematic understanding of the electrochemical corrosion mechanism and behavior of X70 pipe steel in salted soil has remained lacking. In particular, there has been little work to investigate corrosion of the welded steel and the associated structural effects.

In this work, microstructures of pipe steel that resulted from welding (Ref 9) were prepared by different heat treatments, including quenching, air cooling and furnace cooling. Weight loss, electrochemical corrosion measurements, and surface analysis techniques were used to determine the effects of different microstructures of steel on corrosion of X70 steel in an extracted soil solution that simulated the highly salty soil condition. It is anticipated that this work provides essential insight into the mechanism of corrosion of pipe steel and its welds in the highly salted soil.

C.W. Du, X.G. Li, P. Liang, Z.Y. Liu, and **G.F. Jia**, Materials Science and Engineering School, University of Science and Technology Beijing, Beijing 100083, China; and **Y.F. Cheng**, Department of Mechanical and Manufacturing Engineering, University of Calgary, Calgary, AB, Canada T2N 1N4. Contact e-mail: lixiaogang99@263.net.

2. Experimental

The test coupons were fabricated from a sheet of X70 pipe steel, supplied by Bao-Steel Co., China, with a chemical composition (wt.%): C 0.045, Mn 1.48, Si 0.26, S 0.001, P 0.017, Ni 0.16, Cr 0.031, Mo 0.23, Nb 0.033, Cu 0.21, and Fe balance. The coupons were heated to 1200 °C and held at the temperature for 10 min. Heat treatments, including quenching, air cooling and furnace cooling, were then applied to obtain different microstructures. The heat-treated coupons were cut into test specimens with dimensions of $40 \times 20 \times 5$ mm, and were subsequently polished with 800 grit and 1000 grit emery papers, cleaned by distilled water and methanol, and kept in a desiccator for 24 h.

After weighing, the specimens were buried in water-saturated soil that was extracted from 1 m depth where pipelines were buried in the highly salted region in North-West China. During tests, proper amount of de-ionized water was added periodically to keep the soil saturated. The properties and chemical composition of the water-saturated soil is shown in Table 1. The temperature of the soil was controlled at 25 ± 1 °C using a HHS11-Ni2 thermostat water bath. Meanwhile, a NOF bimetallic corrosion meter was used to continuously monitor the corrosion potential of the steel specimen, where the X70 steel specimen was used as working electrode, a saturated calomel electrode (SCE) as the reference electrode and a graphite rod as the counter electrode.

Electrochemical impedance spectroscopy (EIS) measurements were performed periodically on the test electrodes (10×10 mm^2). The AC disturbance signal was 10 mV and the measurement frequency range was 10^5 to 0.01 Hz. ZSimpWin V3.20 impedance analysis software was used to fit the EIS data.

Furthermore, scanning electron microscopy (SEM) was used to observe the surface morphology before and after corrosion tests, and the corrosion products were analyzed by X-ray diffraction (XRD).

3. Results

3.1 Microstructure Observation

The metallographic views of the microstructures of X70 steel with the different heat treatments (quenching, air cooling and furnace cooling) are shown in Fig. 1. It is seen that the microstructure of as-received steel (Fig. 1a) contained mainly pearlite (dark areas) and ferrite (white areas). Ferritic phases were found as irregular nonpolygenic shapes, and grain boundaries were blurry. Upon air cooling, the microstructure of steel (Fig. 1b) contained pearlite and ferrite. The ferrite grains grew further with clear grain boundaries, with the pearlite distributed at grain boundaries. The microstructure obtained by furnace cooling (Fig. 1c) was composed of ferrite with a few granular bainite colonies. The ferrite grains were much larger than those in Fig. 1a. Granular bainite mainly existed at the boundaries of the ferrite region. The steel microstructure obtained by water quenching (Fig. 1d) consisted of fine and well-distributed lath martensite.

Table 1 Chemical composition of the extracted soil solution

pH	Cl^-	SO_4^{2-}	HCO_3^-	Ca^{2+}
8.88	0.1702	0.3064	0.0053	0.0888

3.2 Electrochemical Impedance Spectroscopy Measurements

Figure 2 shows the Nyquist plots of X70 steel with different microstructures buried in soil for 10, 20 and 30 days, respectively. There was a common feature for the measured EIS plots, i.e., a semicircle over the whole test frequency range. Furthermore, at each test time, there was the largest semicircle for as-received steel and the smallest semicircle for quenched steel. The sizes of the semicircle measured on furnace-cooled and air-cooled steels were between these extremes.

An electrochemical equivalent circuit that contains a solution resistance, R_s, in series with a parallel circuit of charge-transfer resistance, R_t, and constant phase element (CPE) for the double-charge layer, was used to fit the impedance data. Figure 3 shows the fitted charge-transfer resistances of the steels as a function of time. The largest charge-transfer resistance was recorded for the as-received steel. Furthermore, R_t increased continuously with time. The second largest charge-transfer resistance occurred for the air-cooled steel, and the difference in R_t for the furnace-cooled steel and water-quenched steel was minor. Moreover, the values of R_t measured at 10, 20 and 30 days on the three heat-treated steel fluctuated, and there was no apparent dependence with test time.

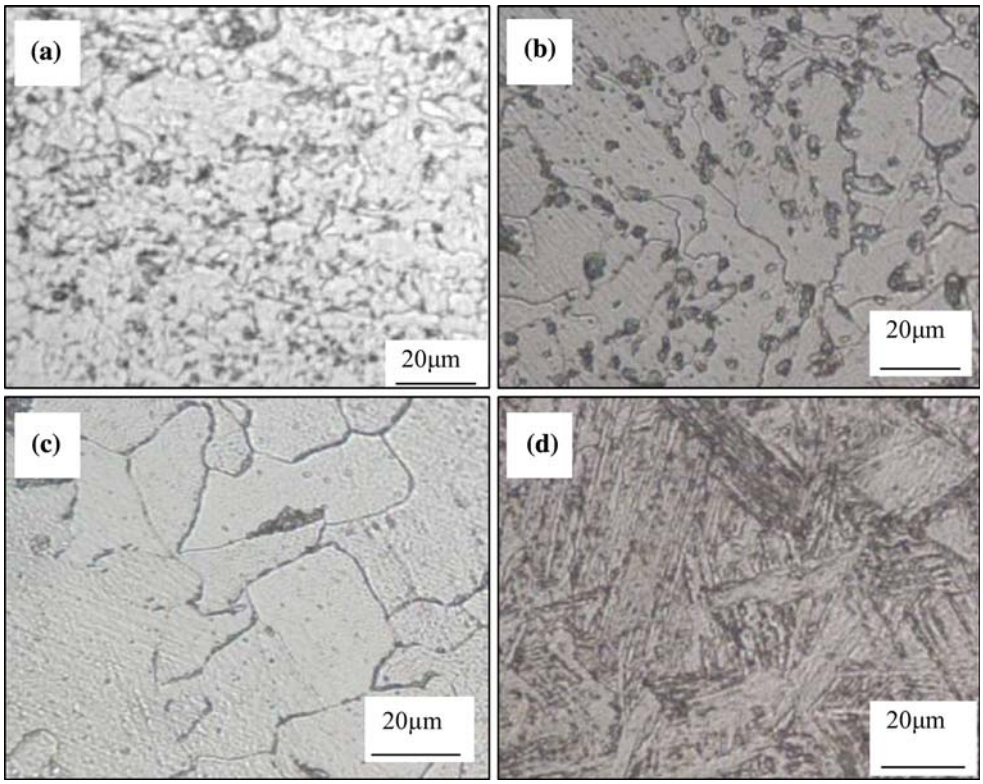

Fig. 1 Metallographic views of the microstructures of X70 steel as-received (a) and with different heat treatments of (b) air-cooling, (c) furnace-cooling and (d) water-quenching

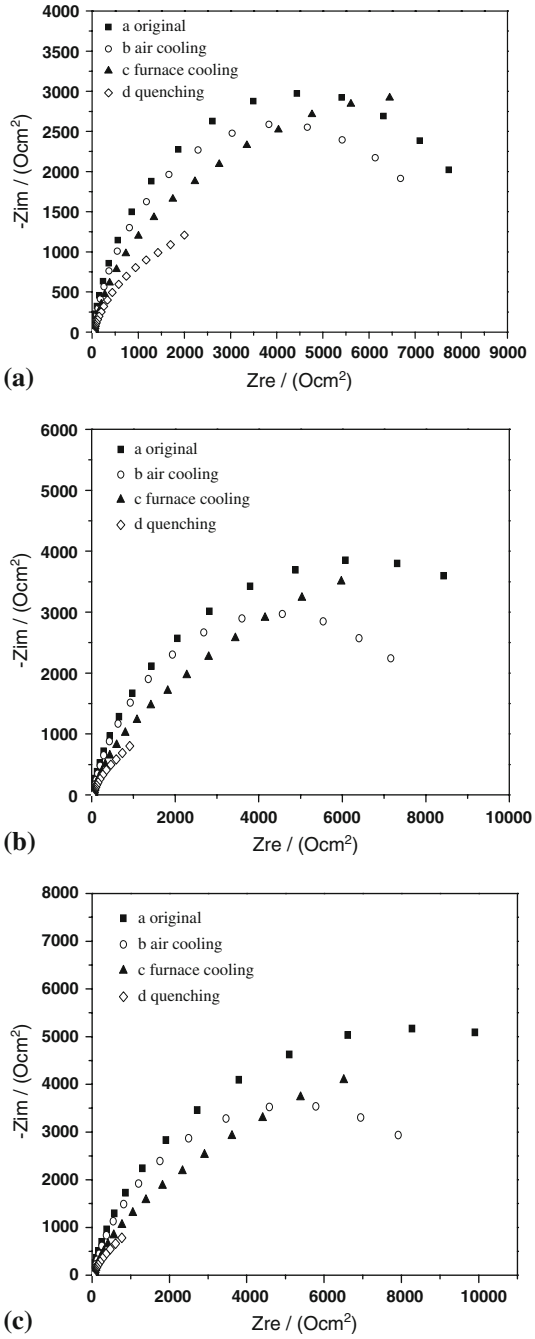

Fig. 2 Nyquist plots of X70 steel with different microstructures that buried in soil for 10 (a), 20 (b) and (c) 30 days

3.3 Corrosion Product Characterization

Figure 4 shows the SEM pictures of corrosion products formed on X70 steel specimens with different microstructures buried in soil for 30 days. It is seen that corrosion product on as-received steel was compact (Fig. 4a), and covered uniformly the specimen surface. Apparently, formation of compact corrosion product layer blocks the approach of corrosive species in the soil, resulting in a low corrosion rate.

For heat-treated steels, the formed corrosion products either have defects or do not cover the whole specimen surface. As shown in Fig. 4(b), corrosion product on the furnace-cooled X70 steel was shaped as strip and feather. Furthermore, the

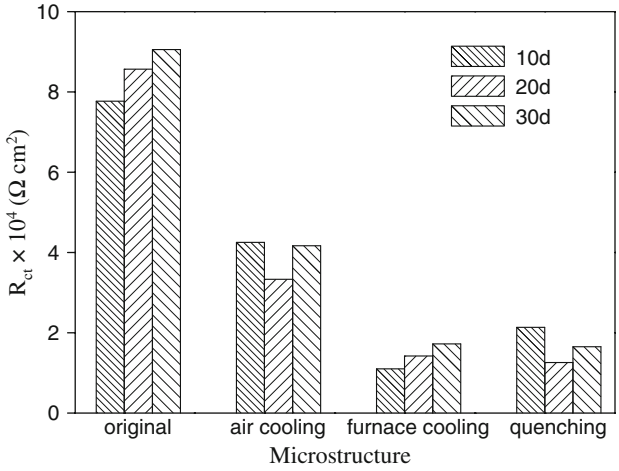

Fig. 3 Charge-transfer resistance of X70 steel with different microstructures as a function of time

corrosion products on X70 steels as a result of air cooling and quenching (Fig. 4c and d) were quite loose, with wider cracks in the oxide layer. Therefore, the different corrosion rates of steels with the different microstructures are attributed to the compactness and completeness of the corrosion product layer formed on the steel surface.

The composition of corrosion products on the various steels in soil was determined by XRD analysis, as shown in Fig. 5. It was found that the corrosion product is basically Fe_2O_3, FeOOH, Fe_3O_4 and FeO. Therefore, if the corrosion product layer is sufficiently compact and complete, it will provide effective protection of the steel from corrosion. The combined analysis of SEM and XRD showed that the different microstructures of steel result in the different physical structure and compactness of corrosion product, rather than different composition, leading consequently to the different corrosion rate of steel.

4. Discussion

4.1 Corrosion Electrochemistry of X70 Steel in Alkaline Soil

The cathodic reaction of X70 steel in aerated, alkaline soil solution is dominated by the reduction of oxygen:

$$3/2O_2 + 3H_2O + 6e \rightarrow 6OH^- \quad \text{(Eq 1)}$$

The anodic process is more complicated, including dissolution of steel and formation of iron compounds with different chemical valences, i.e.:

$$Fe \rightarrow Fe^{2+} + 2e \quad \text{(Eq 2)}$$

$$Fe^{2+} + 2OH^- \rightarrow Fe(OH)_2 \rightarrow FeO + H_2O \quad \text{(Eq 3)}$$

$$4Fe(OH)_2 + O_2 + 2H_2O \rightarrow 4Fe(OH)_3 \quad \text{(Eq 4)}$$

$$4Fe(OH)_2 + O_2 \rightarrow 2Fe_2O_3 + 4H_2O \quad \text{(Eq 5)}$$

$$Fe(OH)_3 \rightarrow FeOOH + H_2O \quad \text{(Eq 6)}$$

XRD results show that all iron oxides, as suggested in Eq 3-6, are possible in alkaline soil. However, different from stable passive film that is usually compact and tightly bonded to the

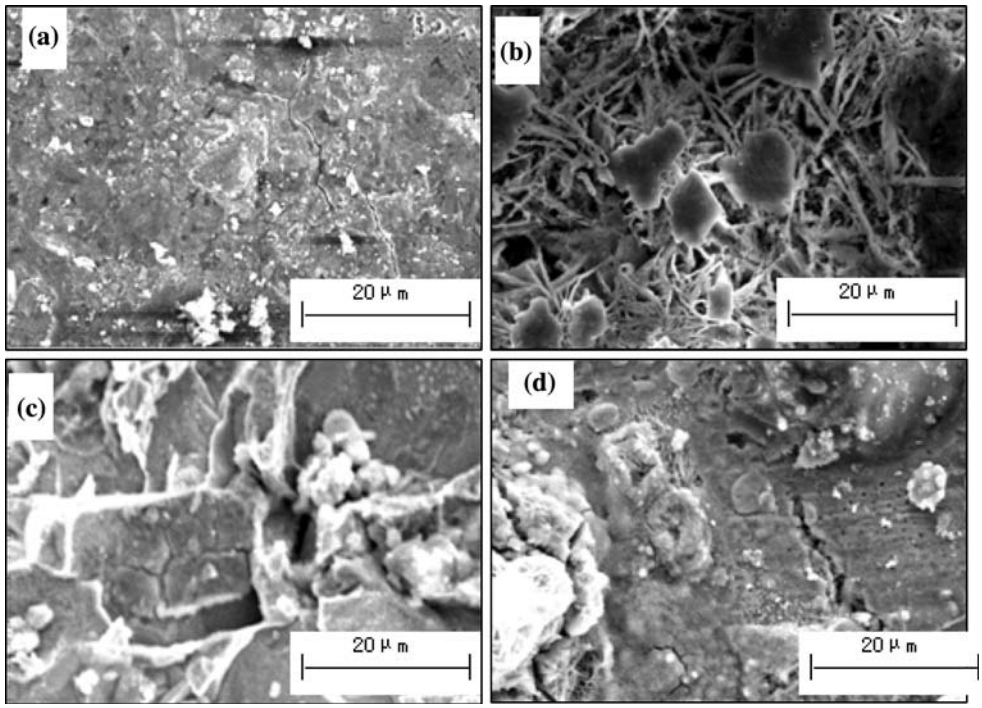

Fig. 4 The surface topographies of X70 steels after tests for 30 days (a) as-received (b) furnace-cooling (c) air-cooling and (d) water-quenching

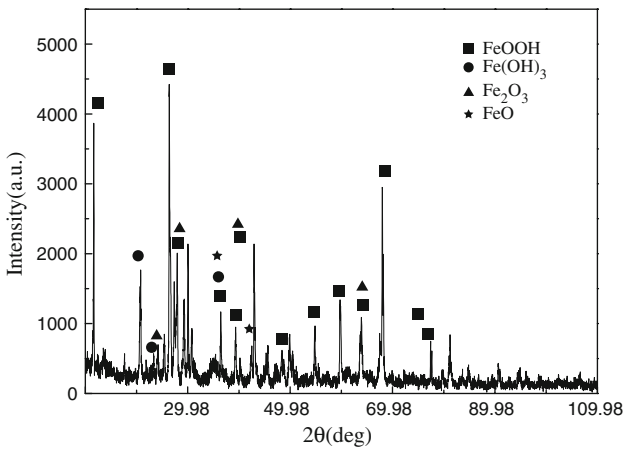

Fig. 5 XRD characterization of corrosion products formed on X70 steel after 30 days of test in soil

steel, these iron oxides exist on the steel surface as a deposited layer because only one time constant was measured on the EIS plots (Fig. 2). Effect of the iron oxide deposit layer on steel corrosion is mainly through a physical blocking effect (Ref 9, 10), which inhibits the access of corrosive species to the steel surface. Therefore, compactness of the deposit layer is a main factor that affects the protectiveness of the steel.

The compact, complete deposit layer formed on as-received steel (Fig. 4a) would inhibit effectively the steel corrosion. Since the deposit layer thickens with time, it is expected that corrosion rate of the steel decreases, as indicated by the increasing charge-transfer resistance (Fig. 3). However, the deposit layers formed on the heat-treated steels are generally porous, with a defective, loose structure (Fig. 4b, c and d), and would not effectively protect the steel. Therefore, the charge-transfer resistances measured on these steels are much lower than that measured on as-received steel, as shown in Fig. 3.

4.2 Effects of Microstructure on Corrosion of Steel

The present work shows that corrosion of steel is affected by its microstructure. In this study, the steels given heat treatments have a higher corrosion rate than the as-received steel (Fig. 3). Upon air cooling, there is more pearlite distributed at the grain boundaries in the ferrite matrix. Since the cementite contained in pearlite is electrochemically more stable than ferrite (Ref 11), a galvanic effect between the cementite and ferrite will enhance the corrosion of the ferrite, resulting in a higher corrosion rate (low charge-transfer resistance).

When the steel is furnace-cooled and water-quenched, bainite and martenite formed. Although a complete understanding of the electrochemical activity of these two phases is still lacking, the present results indicate that they will increase the activity of the steel, as indicated by the decreasing charge-transfer resistance and increasing corrosion rate.

5. Conclusions

The cathodic/anodic reactions of X70 steel in alkaline soil are dominated by oxygen reduction and formation of iron oxides that deposit on the steel surface. The protection the oxide deposit affords the underlying steel is through a physical blocking effect. The structure of the oxide deposit layer plays an essential role in the corrosion of the steel.

The deposit layer formed on the as-received steel is compact and complete and, thus, provides effective protection of the steel. However, the deposit layers on the heat-treated steels are generally loose, porous and defective, and provide only minor protection.

Corrosion of steel is affected by its microstructure. Generally, steels with heat treatments have a higher corrosion rate than the as-received steel. The presence of more pearlite enhances the corrosion of ferrite through a galvanic effect. When the steel contains bainite and martenite, the activity of the steel is further increased.

Acknowledgments

The authors are grateful for the financial support from the National R&D Infrastructure and Facility Development Program of China (Registration Number: 2005DKA10400). Financial support from the National Key Technology R&D Program of China (Registration Number: 2006BAK02B01-06) is also acknowledged.

References

1. L. Niu and Y.F. Cheng, Corrosion Behavior of X-70 Pipe Steel in Near-neutral pH Solution, *Appl. Surf. Sci.*, 2007, **253**, p 8626
2. Y.F. Cheng and L. Niu, Mechanism for Hydrogen Evolution Reaction on Pipeline Steel in Near-neutral pH Solution, *Electrochem. Commun.*, 2007, **9**, p 558
3. M.C. Li and Y.F. Cheng, Corrosion of the Stressed Pipe Steel in Carbonate-bicarbonate Solution Studied by Scanning Localized Electrochemical Impedance Spectroscopy, *Electrochim. Acta*, 2008, **53**, p 2831
4. B. Fang, E.H. Han, J. Wang, and W. Ke, Mechanical and Environmental Influences on Stress Corrosion Cracking of an X-70 Pipeline Steel in Dilute Near-neutral pH Solutions, *Corrosion*, 2007, **63**, p 419
5. M.C. Li and Y.F. Cheng, Mechanistic Investigation of Hydrogen-enhanced Anodic Dissolution of X-70 Pipe Steel and its Implication on Near-neutral pH SCC of Pipelines, *Electrochim. Acta*, 2007, **52**, p 8111
6. C. Du, X. Li, and J. Wu, Corrosion Behavior Comparison of X70 Steel in Three Different Environments, *J. Univ. Sci. Technol. Beijing*, 2004, **26**, p 529
7. X. Li, C. Du, and C. Dong, *Corrosion of X70 Steel*, Science Press, Beijing, 2006
8. Y.-H. Wu, C. Sun, and S.-Q. Zhang, Influence of Soil Humidity on Corrosion Behavior of X70 Pipeline Steel in Saline Soils of Qinghai Salt Lake Region, *Corros. Sci. Protect. Technol.*, 2005, **17**, p 87
9. Y.F. Cheng, Studies of X-65 Pipeline Steel Corrosion in Solutions Containing Carbon Dioxide by Electrochemical Technique, *Bull. Electrochem.*, 2005, **21**, p 503
10. S.L. Asher, B. Leis, J. Colwell, and P.M. Singh, Investigating a Mechanism for Transgranular Stress Corrosion Cracking on Buried Pipelines in Near-neutral pH Environments, *Corrosion*, 2007, **63**, p 932
11. E. Gulbrandsen, R. Nyborg, T. Loland, and K. Nisancioglu, Effects of Steel Microstructure and Composition on Inhibition of CO_2 Corrosion, Corrosion' 2000, NACE, Houston, 2000, paper number 00023